Article:

Article

Analysis of MW-Level Offshore Wind Turbine Generators with Dual Star–Delta Fractional-Slot Windings

Isaac Rudden [1], Guang-Jin Li [1,*], Zi-Qiang Zhu [1], Alexander Duke [2] and Richard Clark [2]

1 Electrical Machines & Drives Group, Department of Electronic and Electrical Engineering, University of Sheffield, Sheffield S10 2TN, UK; iarudden1@sheffield.ac.uk (I.R.); z.q.zhu@sheffield.ac.uk (Z.-Q.Z.)
2 Siemens Gamesa Renewable Energy Limited, North Campus, Broad Lane, Sheffield S3 7HQ, UK; alexander.duke@siemensgamesa.com (A.D.); richard.clark@siemensgamesa.com (R.C.)
* Correspondence: g.li@sheffield.ac.uk

Abstract: This paper investigates the use of fractional-slot concentrated windings (FSCWs) in large-scale (MW level) offshore wind generators. It focuses specifically on a power rating of 3 MW and uses an existing direct-drive synchronous PM machine (DD-SPM) with 480s/160p and dual three-phase integer-slot winding (ISW) as a baseline. A multiple of the common 12s/10p FSCW machine is used that matches the electrical frequency of the ISW machine, yielding a 192s/160p dual three-phase machine. The hybrid star–delta connection has grown increasingly popular owing to its unique harmonic cancellation properties, which can help reduce rotor and PM eddy current losses in FSCW machines. In this paper, two dual three-phase star–delta-wound machines are scaled to 3 MW and included in the investigation. Specifically, a 384s/160p dual three-phase and dual star–delta winding machine, which is a multiplication of the 24s/10p machine, and a 192s/176p dual three-phase and dual star–delta winding machine, which is a multiplication of the 24s/22p machine, are used. These machines are investigated using finite element analysis (FEA) and compared on the basis of their air-gap flux density harmonics, open-circuit electro-motive force (EMF), torque performance, and losses and power. It is found that the proposed 384s/160p dual star–delta winding machine has the best electromagnetic performance of all, with a stator power that is 1.2% greater than that of the baseline ISW machine. However, this machine has a coil pitch of 2 and so loses the manufacturing and fault-tolerant advantage of having concentrated windings. If concentrated windings are desired, then the proposed 192s/176p dual star–delta winding machine is the best choice, with the stator power only 2.6% less than that of the baseline ISW machine, but unfortunately still has significant rotor and PM eddy current losses.

Keywords: concentrated winding; fractional slot; star–delta; PM wind generators

1. Introduction

The rate of wind power installation around the globe is increasing exponentially, with the total worldwide installed capacity reaching 1017 GW at the end of 2023 [1]. Wind power forms a key pillar in the energy decarbonization strategy of most countries aiming to reduce their total emissions in line with the 1.5 °C scenario agreed to in the Paris Agreement [2]. To meet this target, the necessary installed capacity of combined onshore and offshore wind needs to be 3040 GW and 7820 GW by 2030 and 2050, respectively [3]. Offshore wind is projected to provide an increasingly large proportion of the total energy supplied by wind, increasing from just 6% in 2018 to 21% and 35% in 2030 and 2050, respectively [4,5]. Over the last twenty years, the technology used in offshore wind has continued to mature, and the rate of research and development of this technology continues to increase. From 2002 to 2022, there was an average annual increase of 18% in the number of patents filed related to offshore wind power, reaching over 17,000 total applications in 2022 [6].

One of the key components of an offshore wind turbine is the generator, which converts mechanical energy in the wind to electrical energy for the grid. Presently, the

most attractive choice for generator technology in offshore wind turbines is the direct-drive synchronous permanent magnet (DD-SPM) machine [7]. For ease of manufacture, these machines often employ surface-mounted PMs (SPMs), which offer a robust design and structural stability [8]. This requires the use of high-energy magnets like NdFeB to produce a large air-gap flux density [9]. An alternative topology would be the use of buried or interior PMs (IPMs) that can achieve high air-gap flux densities through flux focusing. However, the added complexity and weight of these designs make them unattractive for low-speed wind power applications [10]. These machines also employ two converters driving two separate three-phase winding sets, as this increases the fault tolerance of the overall system; in the event of a converter failure, the turbine can continue to operate, albeit at a reduced capacity [11–13]. These machines are preferable in offshore wind applications to the alternative doubly fed induction generator. These machines have gearboxes that add transmission losses in addition to increasing the failure rate of the turbine when compared to DD-SPM machines [14,15].

The windings in offshore wind power DD-SPM machines are traditionally overlapping windings with an integral number of slots per pole per phase (*spp*) [15]. This requires a distributed winding layout with end windings that overlap. The distributed winding structure yields high efficiency owing to the low rotor and PM eddy current losses [16]. However, distributed windings are difficult to manufacture, especially considering the size and power rating required in modern wind power generators. Furthermore, these distributed windings overlap, which leads to large end-winding losses [16]. The integer-slot machine structure also suffers from large cogging torque, which has to be mitigated in wind power generators by skewing the stator laminates [17], thus sacrificing power. Machines equipped with fractional-slot concentrated windings (FSCWs) have gained increasing popularity in industry as an alternative to this integer-slot winding (ISW) and could soon replace the conventional ISW topology in wind power [18]. Machines equipped with FSCWs have a fractional *spp* number that is ½ lower such that each coil is wound about only a single tooth. This results in concentrated, or non-overlapping, windings. These machines are simpler to wind and so can have higher slot fill factors [19], and the shorter end windings reduce the relative copper loss of this winding type with ISWs [16]. These machines also do not suffer from large cogging torque, so skewing is not necessary [20]. Furthermore, the concentrated windings reduce the mutual inductance between phases and so improve the fault tolerance of these machines [21]; this is of greatest effect when the coils are wound about only alternate teeth (single layer) as opposed to every tooth (double layer) [22]. However, these machines come with a substantial disadvantage in that the simple winding structure results in a large number of unwanted magneto-motive force (MMF) harmonics in the air-gap [23]. These MMF harmonics are loss-causing and induce eddy currents primarily in the rotor and PMs [24,25]. The PM eddy current losses can lead to thermal demagnetization, exacerbated by heat in the rotor caused by the increased eddy current loss there. This is particularly problematic for offshore wind turbine generators, as large current and magnetic loadings are often required, so any added thermal demagnetization risk substantially impacts machine performance.

Work on the use of FSCWs in offshore wind turbines has been carried out before, including work on the design and performance analysis of a modular dual three-phase 3.3 MW offshore wind turbine generator with an FSCW [26]. In this work, Xia et al. investigated different *spp* numbers and their relative performance comparison when looking at onload torque, loss-causing armature MMF harmonics, and cogging torque. They found that an *spp* number of 2/5 or where the slot-pole number follows the relationship $N_s \pm 2 = 2p$ (where N_s and p are the slot number and pole pair number, respectively) results in an FSCW machine that is best for an offshore wind turbine generator. Furthermore, both these choices result in machines that can be operated with two converters as split-phase machines for unwanted MMF harmonic elimination. Xia et al. extended this work to show how the modular structure employed also allows for improved radial cooling through gaps in the stator segments [27]. These works both used measurements from a full-scale

3.3 MW generator and so demonstrate the efficacy of the FSCW design at such a high-power rating. However, they did not compare the chosen topology with an ISW machine topology and so did not show how this winding structure has the potential to replace conventional machines. Work has been carried out on the comparison of FSCWs with ISWs for small-scale wind power applications rated to a few kWs. For 4 kW IPM machines, the FSCWs are found to perform better in terms of cogging torque, power density, torque ripple, and copper loss than similar ISW machines [28]. A comparison of single-layer, double-layer, conventional overlapping, and toroidal windings for 15 kW machines for wind power application was carried out in [29]. After consideration of active mass, rotor and PM eddy current losses, torque ripple, and manufacturing simplicity, the double-layer concentrated winding structure is the most favourable topology. Various works have investigated the impact of the *spp* number on important factors such as demagnetization risk and vibrations in large-scale machines, suggesting that FSCW machines are more susceptible to demagnetization but suffer from fewer vibrations [30,31]. Various other works have included FSCWs in the design of novel wind turbine generators, including axial-flux [32], double-stator [33], and vernier machines [34]. However, the robustness and simplicity of SPMs mean that these alternatives are unlikely to be competitive for offshore wind power applications. Two separate 20 MW wind turbine generators with distributed and concentrated windings are compared in [35], but the authors do not compare the machines' torque performance or the comparative power of these two machines.

Arguably, the most important metric for the comparison of wind turbine generators is the amount of energy that they can produce over their lifetime, which is directly related to the power generated by the machine during operation. Wind turbines are currently designed to last for over 25 years, and so even an incremental increase in the amount of power that the generator can produce would yield a substantial energy increase over the lifetime of the turbine. Therefore, in this paper, a key metric for machine comparison is the stator power, which combines both the torque performance and efficiency of the generator design. The other primary concern, particularly when investigating FSCW machines, is the rotor and PM eddy current losses, which increase the thermal demagnetization risk. There exists a wealth of recent work investigating the application of the hybrid star–delta winding connection to eliminate unwanted armature MMF harmonics and thereby reduce the rotor and PM eddy current losses in FSCW machines [36,37]. In particular, a dual three-phase machine that employs a hybrid star–delta winding connection in each winding set has been shown to exhibit excellent harmonic elimination properties [38–40]. To the authors' best knowledge, no investigations have been conducted into the application of star–delta windings in large-scale wind power generators equipped with FSCWs despite the substantial benefits they could offer to machine performance.

In this paper, a range of 3 MW FSCW machines have been designed and compared with a conventional 3 MW ISW machine. As a second converter is already the convention in offshore wind power, all the machines investigated at the 3 MW scale are also dual three-phase ones. It has been demonstrated extensively in the literature that single-layer FSCW machines suffer from much higher rotor and PM eddy current losses than double-layer FSCW machines [22,25]. As the principal aim of this work is to reduce the rotor and PM eddy current losses, FSCW machines with single-layer windings are not considered. The baseline ISW machine used for this investigation is a 480s/160p machine, and so a suitable starting FSCW machine was deemed to be 192s/160p. This maintains the pole number and, therefore, the electrical frequency and is also a multiple of the common 12s/10p machine that has been studied extensively in the literature. The machines proposed in [38,39] are rated to about 200 W, and the researchers investigated a dual star–delta connection in both 24s/10p and 24s/22p machines. The former yields a machine that no longer has a purely concentrated winding but exhibits excellent MMF harmonic cancellation properties, which substantially reduces the rotor and PM eddy current losses. The latter maintains a concentrated winding and can eliminate all non-torque-producing harmonics but still has notable rotor and PM eddy current losses. In this paper, these two machines are scaled to

3 MW and yield both a 384s/160p (multiple of 24s/10p) machine and a 192s/176p (multiple of 24s/22p) machine. These two slot-pole multiples are studied both as dual three-phase machines with a 30 elec. deg. phase shift between the converters, as well as novel dual star–delta winding machines with a 15 elec. deg. phase shift between the converters.

This work shows that the 192s/160p FSCW dual three-phase machine is not able to match the performance of the baseline ISW machine in terms of stator power or rotor and PM eddy current losses. However, the 384s/160p dual three-phase machine achieves 0.75% higher stator power than the ISW machine with equivalent rotor and PM eddy current losses. By utilizing star–delta windings in the 384s/160p machine, it can achieve a stator power 1.2% higher than that of the ISW machine, although with a notable increase in torque ripple. The 192s/176p dual three-phase machine maintains the advantage of concentrated windings whilst also being an improvement over the 192s/160p machine but still falls behind the ISW in terms of stator power. Again, the dual star–delta winding improves machine performance such that its torque capability is greater than that of the ISW machine, but it still suffers from large rotor and PM eddy current losses with reduced stator power.

2. Machine Winding Layouts

For this investigation into 3 MW FSCW offshore wind power generators, the generator parameters for a 3 MW ISW machine were used as a baseline [15]. These baseline ISW parameters can be seen in Table 1.

Table 1. Parameters of 3 MW ISW.

Slot number	480	Winding layers	1
Pole number	160	Slot-width-to-tooth-width ratio (β)	5/11
Rotor inner radius (m)	2.5	Rated speed (RPM)	15
Air-gap length (mm)	5	Number of turns per coil	12
Magnet length (mm)	15	Number of parallel strings	20
Slot height (mm)	80	Rated current (A_{rms})	160
Yoke height (mm)	40	Magnet-span ratio	0.8
Stack length (m)	1.2	Magnet remanence (T)	1.237

The common 12s/10p machine was selected as the initial FSCW machine for investigation at the 3 MW level. It is evident from the literature that a double-layer winding exhibits a much larger reduction in armature MMF harmonics and so reduced rotor loss when compared with a single-layer winding [22]. As this is a principal concern with the move to an FSCW, a double-layer winding was chosen. All geometric properties in Table 1 were kept the same for the FSCW comparison; the only modifications were those made to the circuit and are summarized in Table 2. To maintain the same number of total turns per phase for the FSCW machine, the number of turns per coil had to be increased to 15. This meant that the number of parallel strings had to be reduced to 16, with 4 coils being in each parallel string. Finally, for a fair comparison of the onload performance it was decided to operate the machines with equal copper losses. One of the principal advantages of an FSCW is the reduced end-winding length, which will allow a higher current to be used while maintaining equal copper loss. In [41], a method for the calculation of coil length for both distributed and concentrated windings is given as

$$L_w = \left(L + k_c \frac{2\pi R_{s-mid}}{N_s} \right) \tag{1}$$

with

$$\begin{cases} k_c = \frac{\pi \tau_s}{2} * coil\ pitch & distributed\ winding \\ k_c = 0.93 & concentrated\ winding \end{cases} \tag{2}$$

where L is the active length of the machine, τ_s is the slot pitch, N_s is the number of stator slots, and $R_{s\text{-}mid}$ is the radius of the middle of the stator slot. The copper losses arising from DC resistance can be calculated using

$$P_{copper} = N_s N_c^2 \rho \frac{L_w}{S k_b} I_{rms}^2 \tag{3}$$

where N_s is the number of slots, N_c is the number of conductors per slot, ρ (Ωm) is the resistivity of copper at room temperature, L_w (m) is the sum of both the active length and end-winding length, S (m^2) is the slot area, k_b is the slot packing factor, and I_{rms} (A) is the phase RMS current. The results of (1) for the 480s/160p and 192s/160p machines can be used in (3) to calculate the copper losses, and then the current of the 192s/160p can be adjusted until the copper losses are equal to those of the ISW machine. This yields a slightly larger rated current for the FSCW machine. The updated circuit properties for the 192s/160p dual three-phase machine can be seen in Table 2.

Table 2. Modifications for 3 MW FSCW.

Slot Number	Winding Layers	Number of Turns per Coil	Number of Parallel Strings	Rated Current (A$_{\text{rms}}$)
192	2	15	16	164.75

Using the dimensions given in Tables 1 and 2, the machine structure and winding layouts for the ISW and FSCW were generated and can be seen in Figure 1.
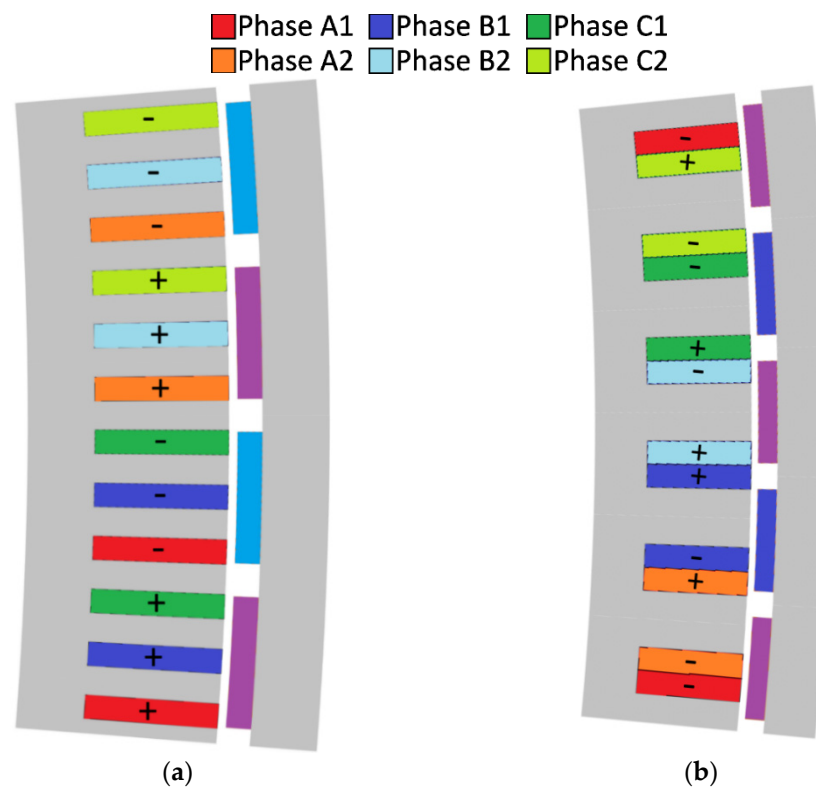
Figure 1. ISW and FSCW baseline machines: (**a**) 480s/160p and (**b**) 192s/160p. Note that the 480s/160p machine shows a full periodic winding section, whereas the 192s/160p machine shows only half a winding section with an antiperiodic boundary.

The star–delta connection works by connecting the ends of the star coils to the terminal nodes of the delta-wound coils. The 30° phase shift between currents in star and delta coils mimics the behaviour of a dual three-phase machine and can be utilized for MMF harmonic

elimination. The difference between the star and hybrid star–delta winding connections, as well as the voltage phasors for the star and delta winding sets, can be seen in Figure 2.
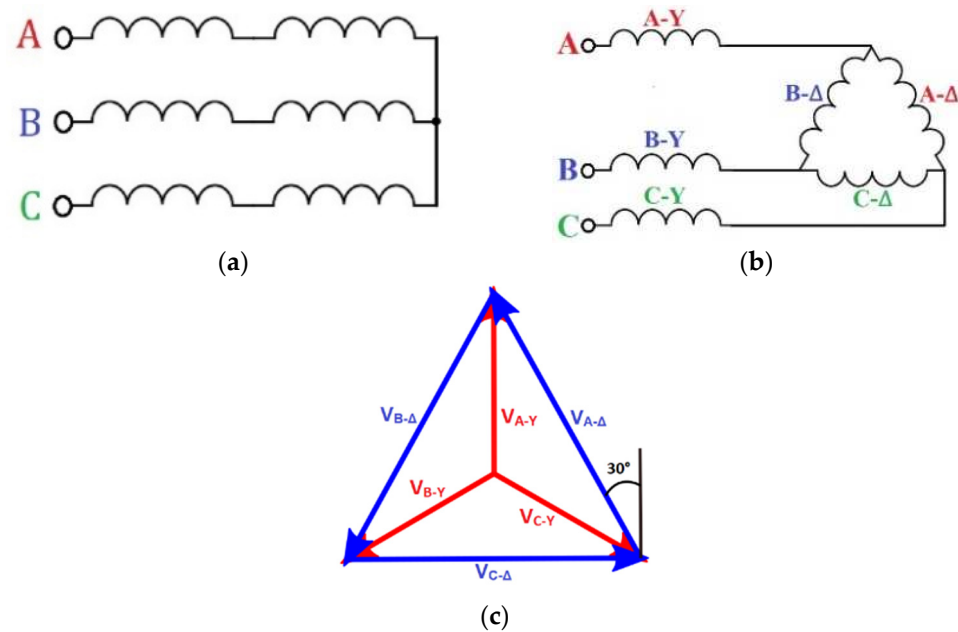
Figure 2. Three-phase winding connections. (**a**) Conventional 3-phase windings, (**b**) star–delta windings, and (**c**) star–delta winding voltage vectors.

In [38], a novel dual three-phase machine was proposed that combined stator shifting and star–delta windings on a baseline 12s/10p machine to produce a 24s/10p machine. The stator shifting employed in the baseline 12-slot machine yielded a 24-slot machine, and applying the same method to the 192s/160p FSCW machine in this study yields a 384s/160p FSW machine. Much like the 192s/160p machine, this topology can use a second converter operating at a 30° elec. deg. phase shift to eliminate the first sub-harmonic and improve machine efficiency. As the number of slots has been doubled, so has the total number of coils, and so the number of turns per coil is reduced to 7.5. By moving to a coil pitch of 2, this machine adopts a semi-overlapping winding structure, and so (1) is used once again for the calculation of the updated end windings. However, this machine is not a fully distributed winding like the ISW machine. Principally, the 384s/160p machine has double-layer windings as opposed to the single-layer windings in the ISW machine. The key difference this has is that the centre of each coil is shifted by a quarter of the slot width on each side. This reduces the end-winding length by a factor of $\beta/2$ and leads to the following equation for winding length in the semi-overlapping 384s/160p machine:

$$L_w = L + k_c \frac{2\pi r_{s-mid}}{N_s}\left(1 - \frac{\beta}{2}\right) \tag{4}$$

where β is the slot–tooth ratio. By following the same process of calculating the rated current for equal copper loss, the rated current is found to be 163.29 A, which lies between the distributed winding and concentrated winding machines, as expected. The winding schematic for such a dual three-phase machine can be seen in Figure 3a. In [39], a second dual three-phase machine was proposed that used star–delta windings to eliminate unwanted harmonics while maintaining a coil pitch of 1. This 24s/22p machine was compared with a 24s/20p dual three-phase machine and was found to have improved electromagnetic performance. Scaling up the 24s/22p machine such that it matched the baseline 3 MW FSCW yielded a 192s/176p dual three-phase machine. Once again, this machine can operate its second converter at a 30 elec. deg. phase shift to eliminate unwanted harmonics and improve machine performance. Since this machine has the same number of slots and

therefore coils as the 192s/160p machine, it also operates at the same rated current. The winding schematic for such a dual three-phase machine can be seen in Figure 3b.
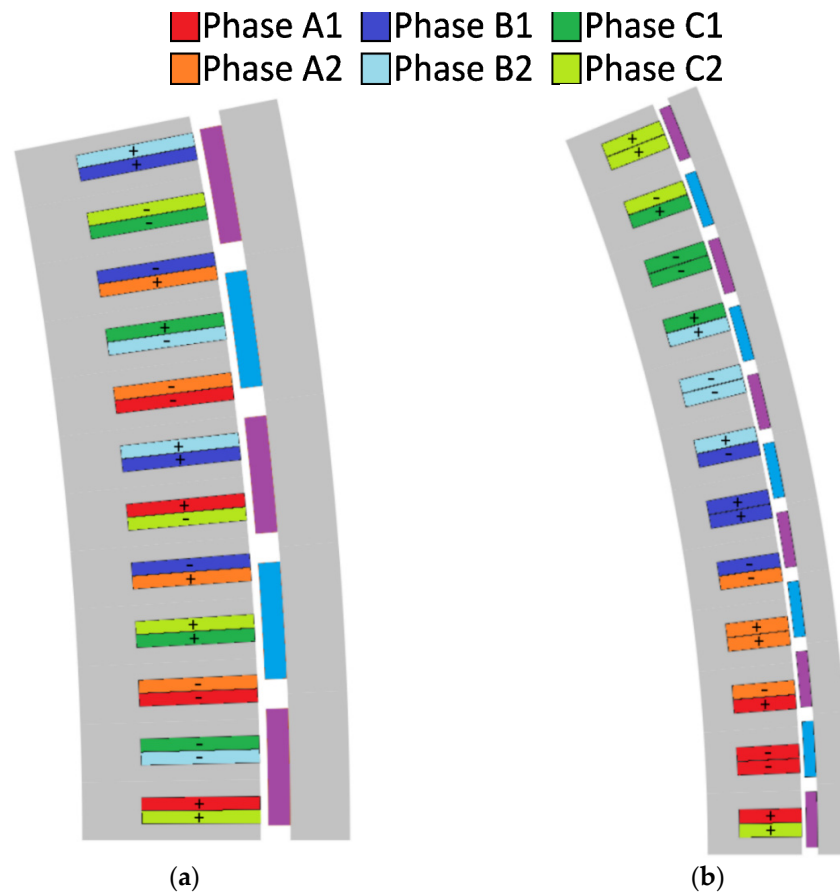

Figure 3. Proposed dual 3-phase machines: (**a**) 384s/160p and (**b**) 192s/176p. In both cases, only half of the winding section with the antiperiodic boundary condition is shown.

As detailed in [39], 24s/10p and 24s/22p are both slot-pole multiples that are feasible solutions for a dual three-phase star–delta-wound machine. In each case, the star–delta windings can be used to artificially create a 30 elec. deg. phase shift between two winding sets in the machine. If star–delta windings are utilized in this way, then the second converter can instead operate a different set of windings at a 15 elec. deg. phase shift for even greater harmonic performance. In [36], it is noted that the number of turns in the delta coils must be $\sqrt{3}$ more than the star coils to achieve an equivalent MMF in the air-gap. The winding layouts for the 384s/160p and 192s/176p dual three-phase machines with star–delta windings can be seen in Figures 4 and 5, respectively. In each case, a schematic is given that shows which coils are wound in star or delta, and a second schematic that shows the interconnections between the delta windings for one of the three-phase sets.

The number of turns for these coils can be seen in Table 3 for the 384s/160p and 192s/176p dual three-phase machines with star–delta windings. It is also explained in [36] that the copper losses remain the same for star and delta coils as the total copper area has been kept constant within the slot. Therefore, these machines are operated at the same rated current as the previous FSW machines. The winding layouts for the 384s/160p and 192s/176p dual three-phase machines with star–delta windings can be seen in Figures 4 and 5, respectively. In each case, a schematic is given that shows which coils are wound in star and which in delta, and a second schematic shows the interconnections between the delta windings for one of the three-phase sets.
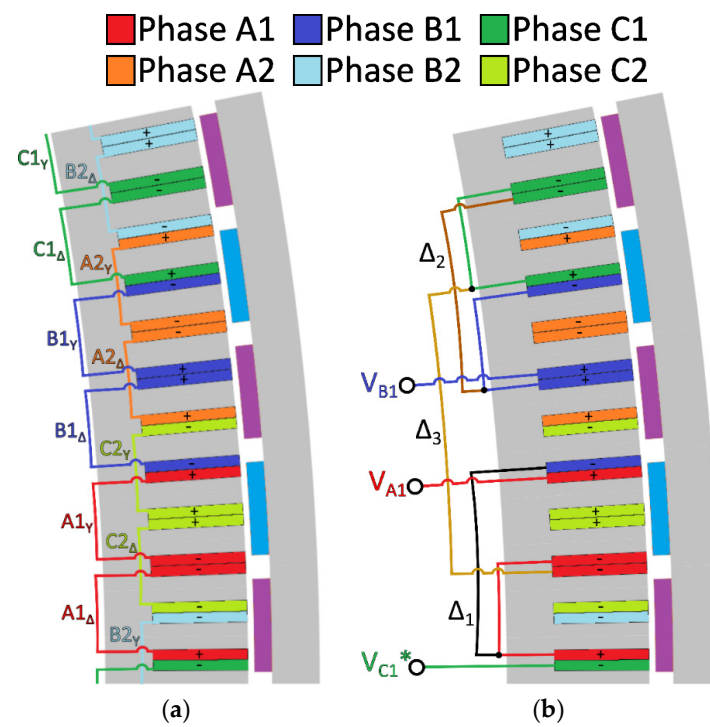
Figure 4. A schematic of 384s/160p dual star–delta winding. (**a**) The coil layout and (**b**) the connections of a single 3-phase set. Note that due to antiperiodic symmetry, V_{c1} is reversed as highlighted by *.
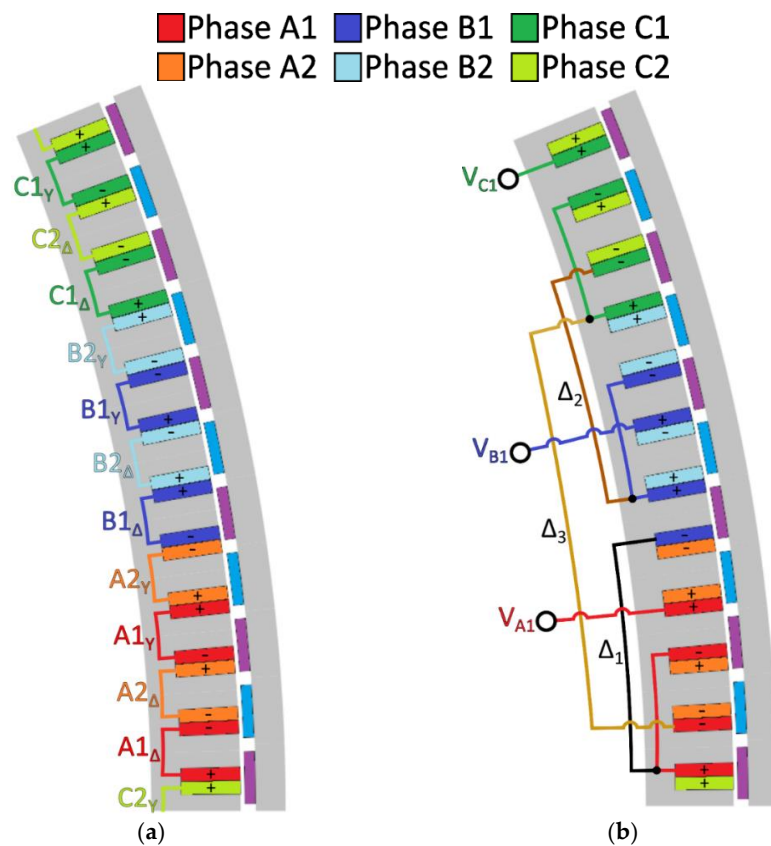
Figure 5. A schematic of 192s/176p dual star–delta winding. (**a**) The coil layout and (**b**) the connections of a single 3-phase set.

Table 3. Star and delta turns per coil.

|	Number of Turns per Star Coil	Number of Turns per Delta Coil	Rated Current (A$_{rms}$)
384s/160p	7.5	13	163.29
192s/176p	15	26	164.75

In summary, the following machines have been selected for this investigation:

- A 480s/160p dual three-phase ISW machine that serves as a baseline conventional distributed winding offshore wind turbine generator [15].
- A 192s/160p dual three-phase FSCW machine that serves as a baseline existing FSCW design for an offshore wind turbine generator [26].
- A 384s/160p dual three-phase FSW machine that shows how the baseline FSCW can be improved by stator shifting.
- A 192s/176p dual three-phase FSCW machine that is an alternative slot-pole multiple to the baseline FSCW machine.
- A 384s/160p dual three-phase FSW machine with star–delta windings that shows how the 384s/160p dual three-phase machine can be further improved with the star–delta connection.
- A 192s/176p dual three-phase FSCW machine with star–delta windings that shows how the 192s/176p dual three-phase machine can be further improved with the star–delta connection.

3. Investigation Setup

3.1. ISW Skewing

The baseline ISW machine is subject to the exceedingly high cogging torque that is inherent in integer-slot machines, owing to the low LCM between the slot number and pole number. Rotor or stator skewing has been shown to be the most effective method for minimizing cogging torque [17,20]. In the case of this paper, skewing is where the stator laminations are sequentially rotated by a miniscule angle along the axial length of the machine, such that the final laminate is rotated by a desired angle with respect to the first laminate. It is demonstrated in [20] that for the optimal cogging torque reduction in an integer-slot machine, a skew angle of one slot pitch must be selected. For the 480s/160p machine, this results in a shift angle of 0.75°, which has been segmented into three axial slices in the software. The ISW machine was modelled in JMAG, and the effects of this skewing on cogging torque and onload torque for the ISW machine under investigation can be seen in Figure 6, with a direct comparison given in Table 4.

(a)

(b)
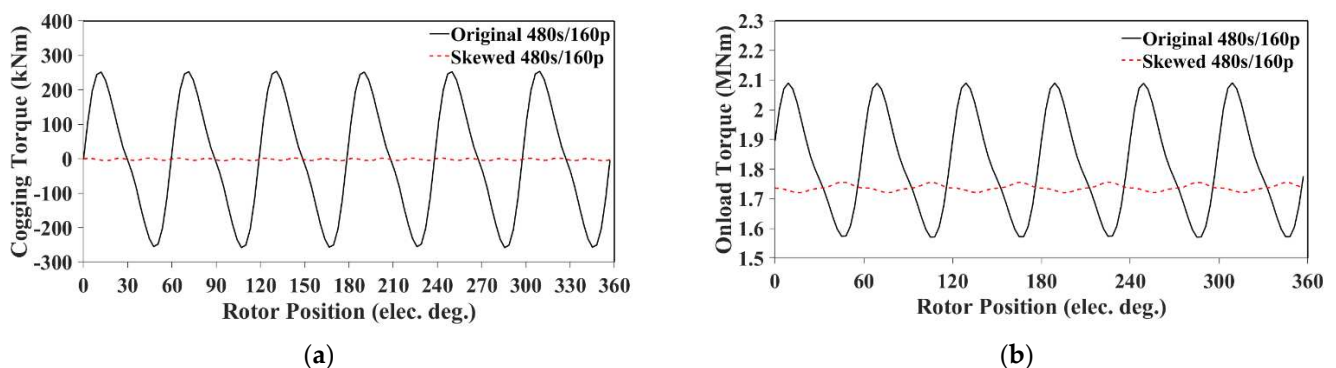
Figure 6. Torque comparison of baseline 480s/160p and skewed 480s/160p machine. (**a**) Cogging torque and (**b**) onload torque.

**Table 4.** Torque performance before and after stator skewing.

	Cogging Torque (kNm)	Average Torque (MNm)	Torque Ripple (kNm)	Torque Ripple (%)	Mech Power (MW)
Original	511.63	1.81	520	28.6	2.85
Skewed	8.59	1.74	36.1	2.08	2.73

By skewing the stator laminates by one slot pitch, the magnitude of the cogging torque has been reduced by over 98%. Although this has reduced the average torque and resulting mechanical power by 3.9%, it is necessary to avoid excessive vibrations that would make the offshore wind turbine generator unstable. With the ISW machine skewed such that the torque performance is more representative of a real-world offshore wind turbine generator, the performance of the proposed FSCW can now be suitably assessed.

3.2. Star–Delta Circuit Modelling

In [38,39], the star–delta connection was used in machine windings to eliminate unwanted harmonics. In these papers, rather than model the full hybrid connection, the star and delta coils were modelled individually and were simply phase-shifted with respect to one another. This was carried out to simplify the model and allow for the investigation of the harmonic elimination property in isolation from any other circuit behaviour. Principally, a delta connection is less favourable than a star connection in an electrical machine due to the presence of a third-order current harmonic that circles within the delta coils. This third-order harmonic can lead to additional copper losses within the stator windings and may also impact torque performance. In a star connection, the neutral point between the coils serves to cancel out this third-order current harmonic.

In this paper, the full star–delta connection was modelled in JMAG, and this section briefly investigates the difference this makes to machine performance when compared with the simple model used in previous works. The machines without the third-order harmonic were created by simply modelling the delta coils as a separate star winding with a 30 elec. deg. phase shift from the star coils. For the machine with third-order harmonic, the full star–delta connection was modelled, which allowed for the circulation of the current within the delta connection. A comparison of onload torque for the machines modelled with and without this third-order circulating current harmonic included can be seen in Figure 7 and Table 5.
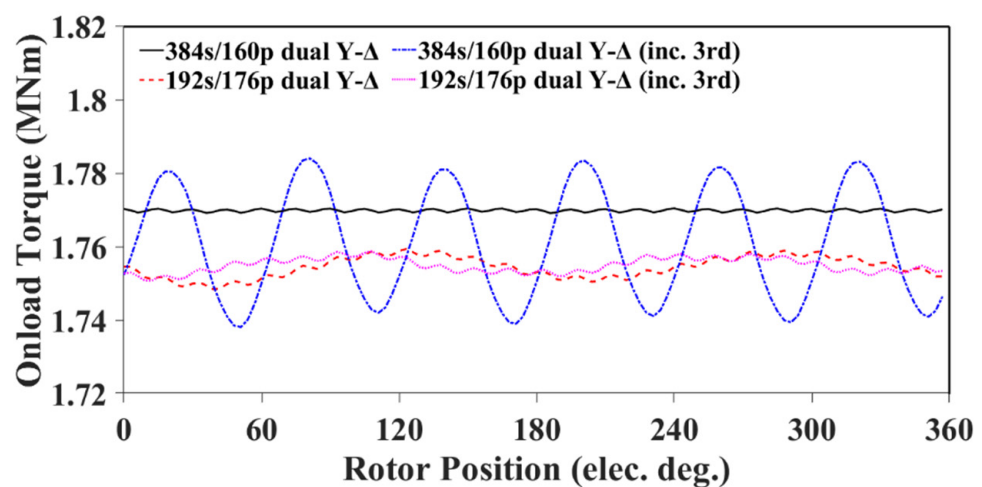
Figure 7. Onload torque comparison of proposed star–delta machines with dual 3-phase only.

Table 5. Torque comparison with and without 3rd-order circulating current harmonic.

|	Average Torque (MNm)	Torque Ripple (kNm)	Torque Ripple (%)	Mech Power (MW)
384s/160p dual Y-Δ	1.77	1.28	0.0721	2.78
384s/160p dual Y-Δ (inc 3rd)	1.76	45.9	2.59	2.77
192s/176p dual Y-Δ	1.75	10.9	0.623	2.76
192s/176p dual Y-Δ (inc 3rd)	1.76	7.97	0.454	2.76

It can be seen that the third-order current harmonic has a detrimental impact on the torque performance of the 384s/160p machine; in particular, it has substantially increased the torque ripple. The third-order current harmonic appears to have limited impact on the torque performance of the 192s/176p dual star–delta machine and, in fact, leads to a slight increase in average torque and a reduction in torque ripple. To understand what might cause this difference between the two machine topologies, the current within example star and delta coils is plotted and decomposed into its constituent harmonic components in Figure 8 and Table 6.
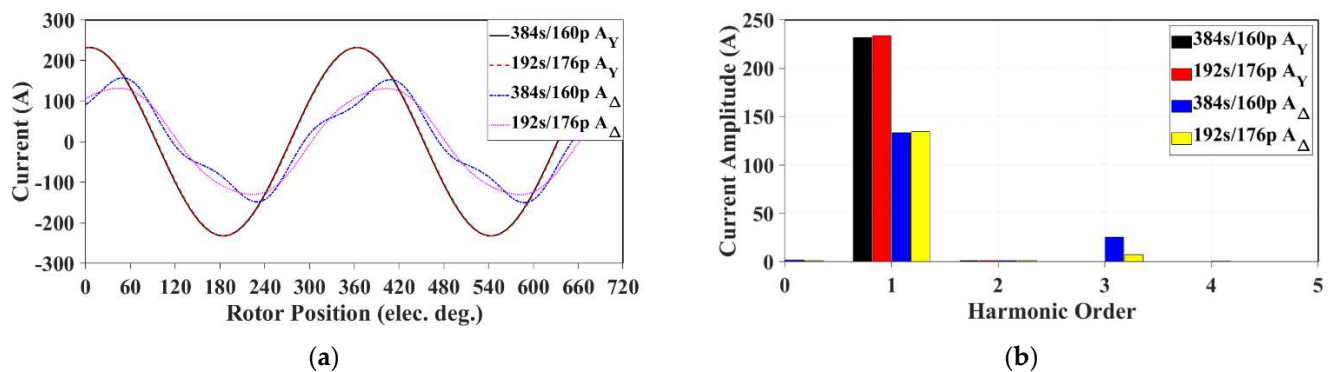
Figure 8. Current comparison within star and delta coils. (**a**) Current waveforms and (**b**) harmonic spectra.

Table 6. Harmonic comparison of current in star and delta coils.

	Fundamental Current Harmonic (A)	3rd-Order Current Harmonic (A)
384s/160p A_Y	231.4	0
192s/176p A_Y	233.4	0
384s/160p A_Δ	133.9	25.3
192s/176p A_Δ	134.7	7.14

The fundamental harmonic component is the same for both the star and delta coils when comparing the 384s/160p and 192s/176p machines. However, the 384s/160p machine has a much larger third-order current harmonic within the delta coils, which is likely the cause of the excessive torque ripple within this machine. The reason for this difference in the third-order harmonic amplitude can be obtained by investigating the EMF induced in the delta coils for both the 384s/160p and 192s/176p machines, as shown in Figure 9 and Table 7. To appropriately compare the two machine structures, the results are given in per unit of the fundamental component of coil induced EMF.
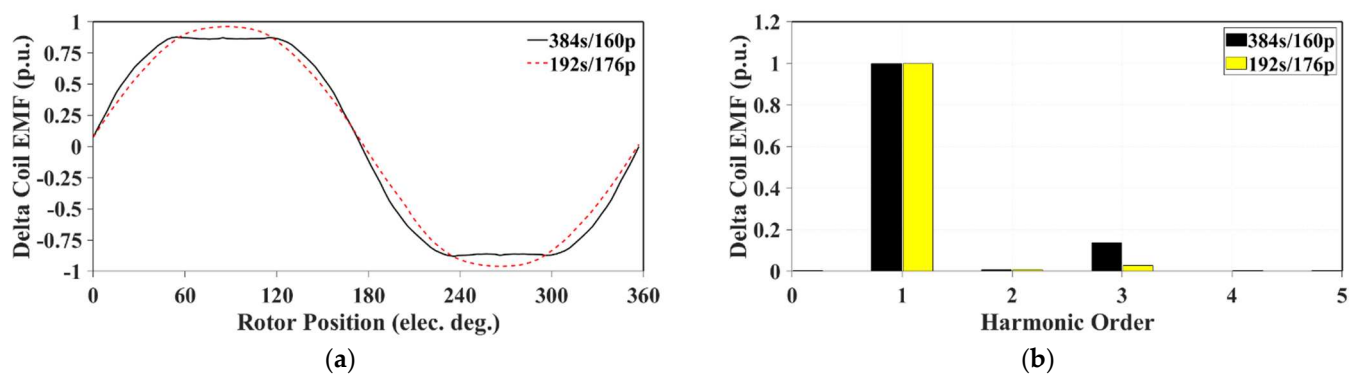
Figure 9. Induced EMF in example delta coils for both machines. (**a**) Coil EMF waveforms and (**b**) EMF spectra.

Table 7. Harmonic comparison of EMF induced in delta coils.

	Fundamental EMF (p.u.)	3rd EMF Harmonic (p.u.)
384s/160p	1.0	0.137
192s/176p	1.0	0.0296

The EMF induced in each coil of the 384s/160p machine includes a much larger third-order harmonic component than in the 192s/176p machine. This can be attributed to the coil pitch of the two machines, specifically how the air-gap permeance might differ between them. The 384s/160p machine uses a coil pitch of two such that the centre of each coil is another slot. This means that when the PM is aligned directly with the coil in a position that would normally induce the peak EMF, it is centred over a slot opening. The reduced air-gap permeance at this point serves to flatten the top of the induced EMF waveform and thus introduce a third-order EMF harmonic. The 192s/176p maintains concentrated windings, meaning that the centre of each coil is an iron tooth. The air-gap permeance at the centre of each tooth is at its maximum and aligns with the peak induced EMF waveform, resulting in a much more sinusoidal induced EMF waveform for the 192s/176p machine. In a star-wound machine, the presence of the third-order harmonic EMF would not be a problem, as the neutral point would serve to prevent a third-order harmonic current. Unfortunately, the delta connection allows for this induced third-order harmonic current to continue circulating within the windings, which causes additional loss and introduces additional torque ripple. It can be deduced from these results that the third-order harmonic is only problematic for the 384s/160p machine owing to the coil pitch of 2. However, it is not detrimental to the 192s/176p machine thanks to the sinusoidal back EMF of the individual coils.

4. FSCW and ISW Comparison

With the preliminary work carried out in the previous section, there are six final machines for comparison. The skewed 480s/160p and 192s/160p dual three-phase machines serve as the baseline ISW and FSCW, respectively. Then, two alternative slot-pole multiples are proposed, i.e., a 384s/160p dual three-phase machine that should have improved harmonic performance but loses the advantage of fully concentrated windings, and a 192s/176p dual three-phase machine that maintains concentrated windings and has a higher pitch factor than the 192s/160p machine but will still have unwanted harmonics. Finally, two novel dual three-phase machines are proposed that utilize the star–delta connection to eliminate additional unwanted harmonics and improve machine performance. These machines are modelled and studied using the JMAG Version 23.0 and OPERA FEA 2023 packages.

4.1. PM and Armature Flux Densities

To identify the expected machine performance, the air-gap flux densities produced by PMs and armature windings are presented in this section. As modelled in [38], the influence of the stator slots on air-gap permeance is reduced with the increasing number of slots. It stands to reason that the magnitude of the open-circuit air-gap flux density is therefore highest in the 480-slot machine, as this has the highest number of slots. To verify this, the four slot-pole multiple machine combinations were modelled in OPERA, and the open-circuit air-gap flux density waveforms were obtained and are presented in Figure 10a, with the corresponding harmonic spectra presented in Figure 10b.


(**a**) (**b**)
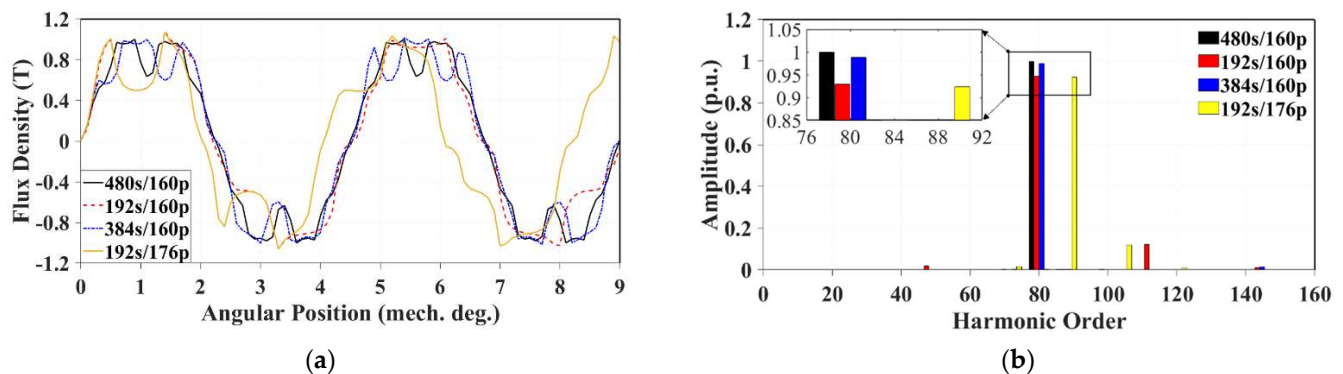
Figure 10. PM flux density comparison. Units given in p.u. of 480s/160p PM flux density. (**a**) Waveforms and (**b**) spectra.

As expected, the machine with the highest fundamental component of the open-circuit air-gap flux density is the ISW. The fundamental component of the open-circuit air-gap flux density in the 384s/160p is only slightly reduced by 1.2%. The 192-slot machines have reductions of 7.0% and 7.6% for the 160-pole and 176-pole machines, respectively. To verify that the harmonic elimination demonstrated in [38,39] on small-scale machines is also applicable to large generators, the six machines under investigation have had their windings sinusoidally excited, with PMs replaced with air. The resulting armature flux densities and harmonic composition can all be seen in Figure 11.

The ISW maintains the largest amplitude of the working harmonic, even despite the rms current being slightly higher for all the FSW machines. The ISW flux density is mostly free of harmonics and has the largest amplitude, a key reason for its extensive use within offshore wind power. The 192s/160p dual three-phase machine has large 80th and 112th harmonics, which correspond to the 5th and 7th harmonics in a 12s/10p dual three-phase machine. The 384s/160p dual star–delta machine achieves the expected harmonic cancellation that was proposed in [38], such that it is free of all but the primary working harmonic. Similarly, the 192s/176p dual star–delta machine has large 88th and 104th harmonics, which correspond to the 11th and 13th harmonics of the 24s/22p dual star–delta machine proposed in [39]. The 88th harmonic is the primary working harmonic and, as discussed in [39], the 104th harmonic becomes torque-producing after flux modulation through the stator teeth. This results in a wind turbine generator with concentrated windings that has eliminated all non-torque-producing armature MMF harmonics. However, this 104th harmonic will unfortunately still induce large eddy currents as it rotates asynchronously with the rotor. Regardless, both dual star–delta-wound machines have succeeded in eliminating one harmonic and increasing the amplitude of the working harmonic when compared with their dual three-phase counterparts.
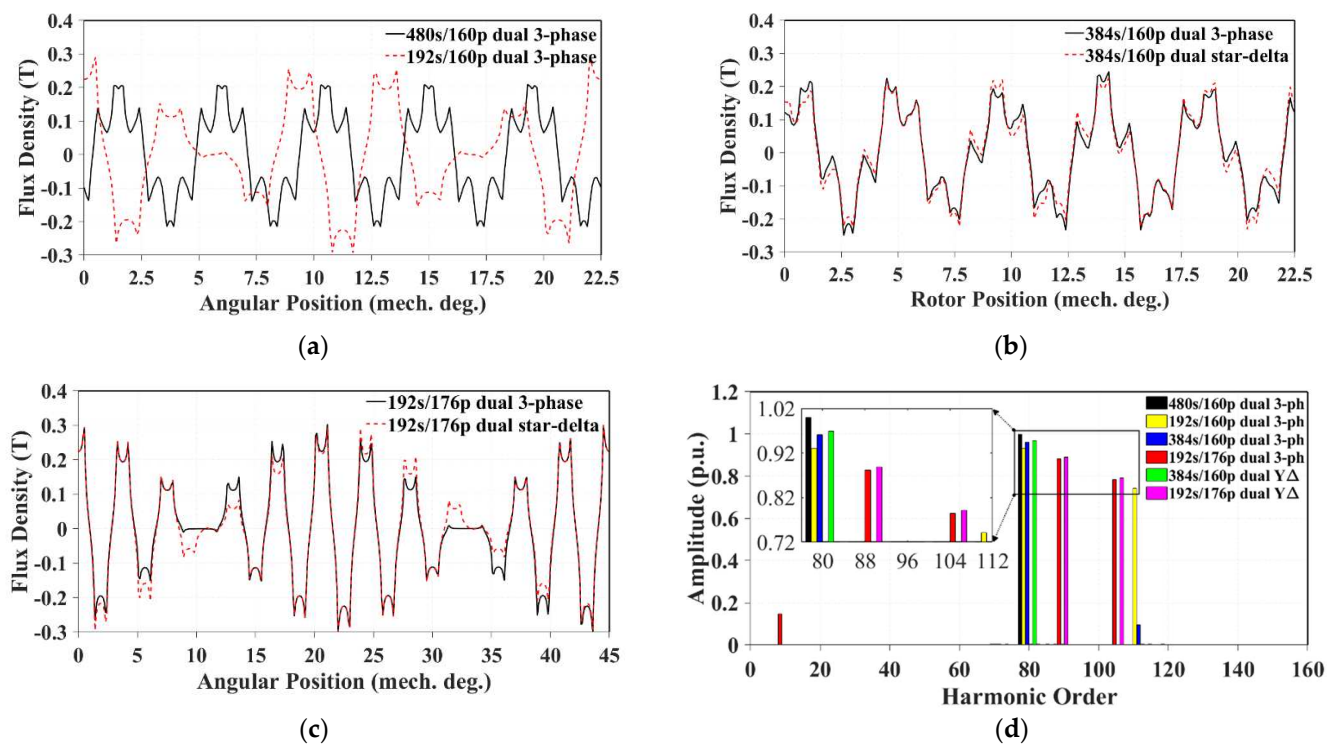
Figure 11. Armature flux density comparison: (**a**) 480s/160p and 192s/160p, (**b**) 384s/160p dual 3-phase and 384s/160p dual star–delta, (**c**) 192s/176p dual 3-phase and 192s/176p dual star–delta, and (**d**) harmonic spectra of all machines. Note all values are given in p.u. of ISW working harmonic.

4.2. Open-Circuit EMF

For the following results, the machines were modelled in JMAG, as this allowed the use of a three-phase current source, which was necessary for the hybrid star–delta machines. As discussed in [38,39], the delta connection makes it impossible to measure the phase voltage of the hybrid star–delta-connected machines. Therefore, for comparison across the six machines, only line EMF has been used. The circuit had to be modified for the baseline FSCW machine such that the number of parallel strings was decreased from 20 to 16. This resulted in more conductors in series for the FSW machines, and so a larger line EMF would be expected. For this comparison, the line EMF of the 480s/160p machine has been multiplied by 1.25 such that it matches the EMF/conductor of the FSW machines under investigation. The waveform and harmonic spectra for the line EMF can be seen in Figure 12, with a breakdown of the fundamental line EMF amplitude given in Table 8.
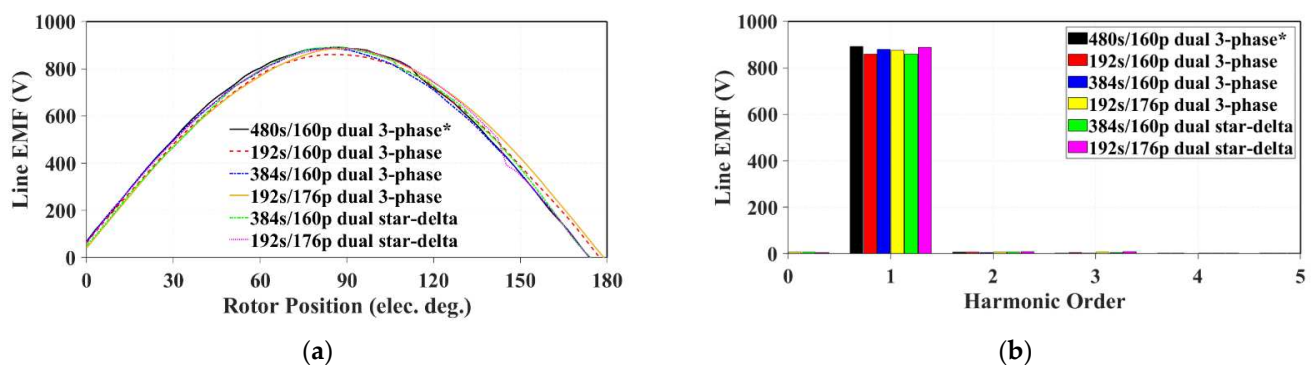
Figure 12. A line EMF comparison of the investigated machines. (**a**) Waveforms and (**b**) spectra. Note that the 480s/160p line EMF has been multiplied by 1.25 for a fair comparison. * means that this machine is used as a reference.

Table 8. Line EMF fundamental harmonic comparison.

	Line EMF Fundamental (V)
480s/160p dual 3-phase *	891.5
192s/160p dual 3-phase	858.3
384s/160p dual 3-phase	879.6
192s/176p dual 3-phase	875.1
384s/160p dual star–delta	858.3
192s/176p dual star–delta	888.0

* means that this machine is used as a reference.

The 480s/160p dual three-phase machine produces the largest open-circuit fundamental line EMF at rated speed. Following this, the 192s/176p dual star–delta machine has the second highest line EMF fundamental component, just 0.4% less than that of the ISW machine. Unfortunately, the 384s/160p dual star–delta machine does not achieve as high a line EMF fundamental as the 384s/160p dual three-phase machine, which can likely be attributed to the third harmonic current circulating within the delta windings.

4.3. Torque Performance

In this investigation, there are six machines but only four slot-pole number combinations. The cogging torque for the ISW machine has already been shown in Section 3.1, but it is displayed again here for comparison with the three FSW slot-pole number combinations and can be seen in Figure 13 and Table 9. Table 10 summarizes the onload torque performance of different investigated machines.
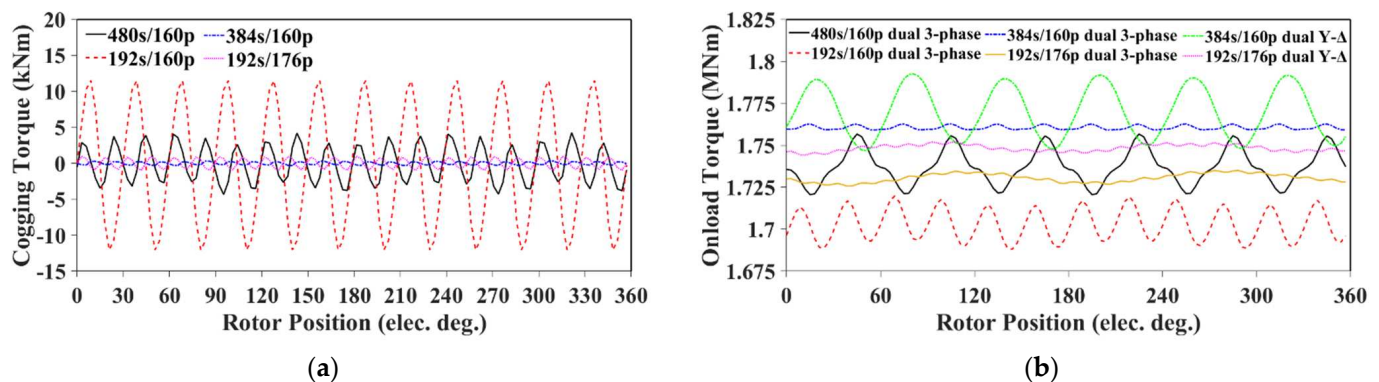
Figure 13. Torque comparison. (**a**) Cogging torque and (**b**) onload torque.

Table 9. Cogging torque comparison.

	480s/160p	192s/160p	384s/160p	192s/176p
Cogging torque (kNm)	8.59	23.6	0.618	1.94

Table 10. Onload torque comparison.

	Average Torque (MNm)	Torque Ripple (KNm)	Torque Ripple (%)	Mech Power (MW)
480s/160p dual 3-phase	1.74	36.1	2.08	2.73
192s/160p dual 3-phase	1.71	31.8	1.86	2.69
384s/160p dual 3-phase	1.75	3.67	0.209	2.75
192s/176p dual 3-phase	1.74	9.42	0.542	2.73
384s/160p dual Y-Δ	1.76	45.9	2.61	2.77
192s/176p dual Y-Δ	1.76	7.97	0.454	2.76

The 192s/160p and 192s/176p dual three-phase machines are unable to exceed the torque performance of the 480s/160p dual three-phase machine and so do not suggest that concentrated windings could offer an alternative to the ISW for wind power applications. However, by utilizing the star–delta connection, the 192s/176p dual star–delta machine can exceed the torque capability while still having concentrated windings. The 384s/160p dual three-phase machine achieves 0.9% higher onload torque than the 480s/160p dual three-phase machine, and this is increased to 1.4% by utilizing a dual star–delta connection. However, the third-order circulating current in the delta windings leads to the largest torque ripple of all the investigated machines. Despite this, the torque ripple is not too much larger than the 480s/160p machine so could still be an attractive option for offshore wind power. The machines have also been operated at incremental phase currents up to twice the rated current, and the resulting average torque and torque ripple coefficients are plotted against the phase current in Figure 14.
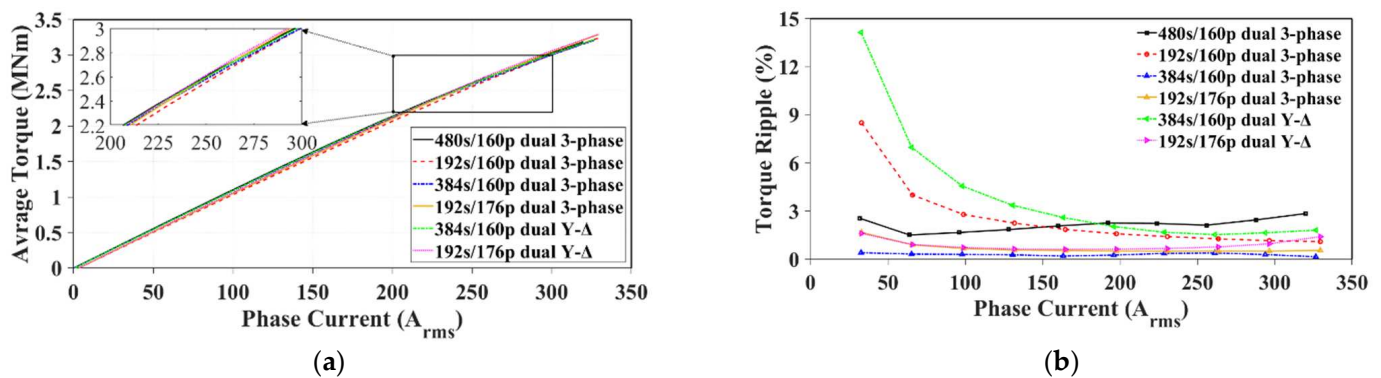
Figure 14. Torque performance plotted against increasing phase current. (**a**) Average torque and (**b**) torque ripple coefficient.

As highlighted in Figure 14a, once the current reaches approximately 1.5 times the rated current, the concentrated windings begin to outperform the ISW or semi-overlapping winding machines. This is attributed to the larger teeth in the 192-slot machines, which can sustain higher phase currents before becoming overly saturated with flux. In particular, the machine that has the greatest torque capability from 1.5 times the rated current is the 192s/176p dual star–delta winding machine. The torque ripple coefficients of most of the machines remain within about 3% for all phase currents. However, the 192s/160p dual three-phase machine has a large torque ripple coefficient at low phase currents, which can be attributed to the large cogging torque evident in Figure 13a. Similarly, the 384s/160p dual star–delta machine has a very large torque ripple coefficient at low phase currents of nearly 15%. This is likely caused by the third-order circulating current harmonic in the delta coils discussed in Section 3.2.

4.4. Losses and Efficiency

For a final comparison of the six machines, the losses and efficiency were calculated to assess the stator power. This is a direct indication of the comparative energy yield of each machine and so a critical metric for the comparison of the machines' application in offshore wind power. The copper losses were calculated using (3), with the rated current being slightly different in order to maintain the same copper loss for all machines. The concentrated winding machines are likely to have the highest slot filling factor, which would improve machine performance. However, the double-layer winding structure increases the amount of insulation needed in the slot when compared with the single-layer ISW machine. As it was not possible to determine the difference that these attributes would have on the slot filling factor, a value of 0.6 was used for all machines [15]. This resulted in a DC copper loss of 57.3 kW for all star-wound machines. For the star–delta-wound machines, the third-order harmonic current circulating in the delta coils obtained in Table 6

has been used for the calculation of additional copper loss. Thus, the total copper loss of the 384s/160p and 192s/176p dual star–delta winding machines is 58.3 kW and 57.4 kW, respectively. For the remaining losses, a laminated stator was used, as this is essentially a necessity for these wind power generators. A solid iron rotor core was used owing to the simple structure, and it provides added mechanical stiffness when an external rotor structure is used. Furthermore, as one of the principal aims of this paper is to investigate the impact of different winding structures on rotor and PM eddy current losses, the solid iron rotor core was used so that the worst-case scenario for eddy current loss could be evaluated. For this reason, PM segmentation is also not considered in the model. These losses have all been calculated using JMAG, and the results are presented in Table 11.

Table 11. Comparison of losses and efficiency.

	Stator Loss (kW)	Rotor Loss (kW)	PM Loss (kW)	Efficiency (%)	Stator Power (MW)
480s/160p dual 3-phase	24.3	0.290	2.92	96.89	2.64
192s/160p dual 3-phase	17.9	49.4	45.6	93.66	2.51
384s/160p dual 3-phase	23.6	1.64	5.98	96.78	2.66
192s/176p dual 3-phase	18.0	64.4	45.1	93.23	2.55
384s/160p dual Y-Δ	23.6	2.47	6.13	96.73	2.68
192s/176p dual Y-Δ	18.4	59.4	46.9	93.40	2.57

The results show that the 384s/160p dual three-phase and dual star–delta winding machines produce 0.75% and 1.2% more power than the 480s/160p dual three-phase machine. If maximizing the stator power was the only objective, then the 384s/160p dual star–delta winding machine would be the preferred choice. These machines both have minimal rotor and PM eddy current losses, which also makes them an attractive choice when considering the thermal demagnetization risk.

Unfortunately, none of the machines that maintain concentrated windings match the stator power of the 480s/160p dual three-phase machine. Additionally, the concentrated winding also leads to much larger rotor and PM eddy current losses. The baseline 192s/160p dual three-phase FSCW machine produces 4.9% less power than the 480s/160p, but by changing the slot-pole multiple, this difference can be reduced. The 192s/176p dual three-phase machine produces 3.8% less power than the ISW machine, and by utilizing a dual star–delta connection, this difference can be reduced to only 2.6%. If a concentrated winding structure is critical and the rotor and PM eddy current losses are within an acceptable range, then the 192s/176p dual star–delta winding machine is the obvious choice.

5. Conclusions

This paper investigated the use of machines equipped with FSWs for use in offshore wind turbine generators. The main objective was to identify an FSCW machine that could produce a similar or even greater amount of power to a conventional ISW machine whilst also keeping rotor and PM eddy current losses to a minimum. A 480s/160p dual three-phase machine was used as an ISW baseline, and the common 12s/10p FSCW machine was multiplied to give a 192s/160p dual three-phase machine that served as an initial FSCW comparison. Techniques developed in previous work were then used to produce a stator shifted 384s/160p dual three-phase machine, a 384s/160p dual star–delta winding machine, a 192s/176p dual three-phase machine, and a 192s/176p dual star–delta winding machine. These machines were then compared extensively, including sections on air-gap flux density harmonics, open-circuit line EMF, torque performance, and efficiency and power.

Unfortunately, an FSCW machine was not identified that could match the stator power of the baseline ISW machine. However, the 192s/176p dual star–delta winding machine proposed in this work was found to have the highest stator power of all FSCW machines (only 2.6% less than the ISW machine and 2.4% more than the 192s/160p dual three-phase FSCW machine). These machines, of course, still benefit from the other key advantages of

concentrated windings, such as the ease of manufacture and higher fault tolerance. Furthermore, the same slot filling factor was used for all machines investigated. Concentrated windings can achieve a higher slot filling factor than distributed windings, and future work should include this in the analysis, as it would greatly improve the comparative performance of the concentrated winding machines. Furthermore, if a laminated rotor core structure is used, in addition to conventional PM segmentation methods, the rotor and PM eddy current losses in these concentrated winding machines could be greatly reduced.

The two 384s/160p machines were able to produce more power than the baseline ISW machine with equivalent rotor and PM eddy current losses. The 384s/160p dual star–delta winding machine proposed in this work showed the best performance and was able to produce 1.2% more power than the presently employed ISW with only a 0.53% increase in the torque ripple coefficient. This work demonstrates that dual star–delta windings can be utilized to improve the efficacy of FSW machines in offshore wind turbine generators and therefore proposes two prospective machine topologies:

- If annual energy production is the most critical consideration, then the 384s/160p dual star–delta winding machine is the best solution, with a 1.2% increase in stator power compared with the existing ISW baseline machine.
- If a concentrated winding structure is desired, then the 192s/176p dual star–delta winding machine is the best solution, with only a 2.6% reduction in stator power compared to the existing ISW baseline machine.

Author Contributions: Writing—original draft, I.R.; writing—review and editing, and supervision, G.-J.L. and Z.-Q.Z.; funding acquisition and supervision, A.D. and R.C. All authors have read and agreed to the published version of the manuscript.

Data Availability Statement: The original contributions presented in the study are included in the article, further inquiries can be directed to the corresponding author.

Conflicts of Interest: Authors Alexander Duke and Richard Clark were employed by the company Siemens Gamesa Renewable Energy Limited. The remaining authors declare that the research was conducted in the absence of any commercial or financial relationships that could be construed as a potential conflict of interest.

References

1. IRENA. *Renewable Capacity Statistics 2024*; IRENA: Abu Dhabi, United Arab Emirates, 2024.
2. UNFCC. Paris Agreement. 2015. Available online: https://unfccc.int/sites/default/files/english_paris_agreement.pdf (accessed on 16 May 2024).
3. IRENA. *World Energy Transitions Outlook 2023: 1.5° Pathway*; IRENA: Abu Dhabi, United Arab Emirates, 2024.
4. IRENA. *Future of Wind*; IRENA: Abu Dhabi, United Arab Emirates, 2019.
5. IRENA. *Offshore Renewables: An action Agenda for Deployment*; IRENA: Abu Dhabi, United Arab Emirates, 2021.
6. IRENA. *Offshore Wind Energy: Patent Insight Report*; IRENA: Abu Dhabi, United Arab Emirates, 2023.
7. Bensalah, A.; Barakat, G.; Amara, Y. Electrical generators for large wind turbine: Trends and challenges. *Energies* **2022**, *15*, 6700. [CrossRef]
8. Mueller, M.; Zavvos, A. 1—Electrical generators for direct drive systems: A technology overview. In *Electrical Drives for Direct Drive Renewable Energy Systems*; Mueller, M., Polinder, H., Eds.; Woodhead Publishing: Sawston, UK, 2013; pp. 3–29.
9. Bhuiyan, N.A.; Mcdonald, A. Optimization of offshore direct drive wind turbine generators with consideration of permanent magnet grade and temperature. *IEEE Trans. Energy Convers.* **2019**, *34*, 1105–1114. [CrossRef]
10. Mcdonald, A.; Bhuiyan, N.A. On the optimization of generators for offshore direct drive wind turbines. *IEEE Trans. Energy Convers.* **2017**, *32*, 348–358. [CrossRef]
11. Gjerde, S.S.; Olsen, P.K.; Ljokelsoy, K.; Undeland, T.M. Control and fault handling in a modular series-connected converter for a transformerless 100 kv low-weight offshore wind turbine. *IEEE Trans. Ind. Appl.* **2014**, *50*, 1094–1105. [CrossRef]
12. Duran, M.J.; Prieto, I.G.; Bermudez, M.; Barrero, F.; Guzman, H.; Arahal, M.R. Optimal fault-tolerant control of six-phase induction motor drives with parallel converters. *IEEE Trans. Ind. Electron.* **2016**, *63*, 629–640. [CrossRef]

13. Gonzalez-Prieto, I.; Duran, M.J.; Che, H.S.; Levi, E.; Bermudez, M.; Barrero, F. Fault-tolerant operation of six-phase energy conversion systems with parallel machine-side converters. *IEEE Trans. Power Electron.* **2016**, *31*, 3068–3079. [CrossRef]
14. Echavarria, E.; Hahn, B.; van Bussel, G.; Tomiyama, T. Reliability of wind turbine technology through time. *Fraunhofer IWES* **2008**, *130*, 031005. [CrossRef]
15. Polinder, H.; Van Der Pijl, F.F.A.; De Vilder, G.-J.; Tavner, P.J. Comparison of direct-drive and geared generator concepts for wind turbines. *IEEE Trans. Energy Convers.* **2006**, *21*, 725–733. [CrossRef]
16. El-Refaie, A.M. Fractional-slot concentrated-windings synchronous permanent magnet machines: Opportunities and challenges. *IEEE Trans. Ind. Electron.* **2010**, *57*, 107–121. [CrossRef]
17. Islam, R.; Husain, I.; Fardoun, A.; Mclaughlin, K. Permanent-magnet synchronous motor magnet designs with skewing for torque ripple and cogging torque reduction. *IEEE Trans. Ind. Appl.* **2009**, *45*, 152–160. [CrossRef]
18. El-Refaie, A. Fractional-slot concentrated-windings: A paradigm shift in electrical machines. In Proceedings of the 2013 IEEE Workshop on Electrical Machines Design, Control and Diagnosis (WEMDCD), Paris, France, 11–12 March 2013; IEEE: Piscataway, NJ, USA, 2013.
19. Jack, A.G.; Mecrow, B.C.; Dickinson, P.G.; Stephenson, D.; Burdess, J.S.; Fawcett, N.; Evans, J.T. Permanent-magnet machines with powdered iron cores and prepressed windings. *IEEE Trans. Ind. Appl.* **2000**, *36*, 1077–1084. [CrossRef]
20. Zhu, Z.Q.; Howe, D. Influence of design parameters on cogging torque in permanent magnet machines. *IEEE Trans. Energy Convers.* **2000**, *15*, 407–412. [CrossRef]
21. El-Refaie, A.M.; Zhu, Z.Q.; Jahns, T.M.; Howe, D. Winding inductances of fractional slot surface-mounted permanent magnet brushless machines. In Proceedings of the 2008 IEEE Industry Applications Society Annual Meeting, Edmonton, AB, Canada, 5–9 October 2008.
22. Ishak, D.; Zhu, Z.Q.; Howe, D. Comparison of pm brushless motors, having either all teeth or alternate teeth wound. *IEEE Trans. Energy Convers.* **2006**, *21*, 95–103. [CrossRef]
23. Bianchi, N.; Bolognani, S.; Pre, M.D.; Grezzani, G. Design considerations for fractional-slot winding configurations of synchronous machines. *IEEE Trans. Ind. Appl.* **2006**, *42*, 997–1006. [CrossRef]
24. Atallah, K.; Howe, D.; Mellor, P.H.; Stone, D.A. Rotor loss in permanent magnet brushless AC machines. *IEEE Trans. Ind. Appl.* **2000**, *36*, 1612–1618.
25. Bianchi, N.; Fornasiero, E. Impact of mmf space harmonic on rotor losses in fractional-slot permanent-magnet machines. *IEEE Trans. Energy Convers.* **2009**, *24*, 323–328. [CrossRef]
26. Xia, J.; Tian, D.; Gao, Y.; Wang, W.; Fan, W. Electromagnetic design and performance analysis of large-scale offshore wind generators with modular fractional-slot concentrated winding. *Energy Rep.* **2023**, *10*, 186–201. [CrossRef]
27. Xia, J.; Tian, D.; Liu, J.-W.; Li, J.-H.; Li, P. Coupled airflow-thermal network model for large-scale offshore wind generators with modular fractional-slot concentrated winding. *IEEE Trans. Energy Convers.* **2023**, *38*, 899–913. [CrossRef]
28. Ahsanullah, K.; Dutta, R.; Rahman, M.F. Analysis of low-speed ipmms with distributed and fractional slot concentrated windings for wind energy applications. *IEEE Trans. Magn.* **2017**, *53*, 3101710. [CrossRef]
29. Potgieter, J.H.J.; Kamper, M.J. Design optimization of directly grid-connected pm machines for wind energy applications. *IEEE Trans. Ind. Appl.* **2015**, *51*, 2949–2958. [CrossRef]
30. Chen, H.; Qu, R.; Li, J.; Li, D. Demagnetization performance of a 7 mw interior permanent magnet wind generator with fractional-slot concentrated windings. *IEEE Trans. Magn.* **2015**, *51*, 8205804. [CrossRef]
31. Valavi, M.; Nysveen, A.; Nilssen, R.; Lorenz, R.D.; Rolvag, T. Influence of pole and slot combinations on magnetic forces and vibration in low-speed pm wind generators. *IEEE Trans. Magn.* **2014**, *50*, 8700111. [CrossRef]
32. Brisset, S.; Vizireanu, D.; Brochet, P. Design and optimization of a nine-phase axial-flux pm synchronous generator with concentrated winding for direct-drive wind turbine. *IEEE Trans. Ind. Appl.* **2008**, *44*, 707–715. [CrossRef]
33. Gul, W.; Gao, Q.; Lenwari, W. Optimal design of a 5-mw double-stator single-rotor pmsg for offshore direct drive wind turbines. *IEEE Trans. Ind. Appl.* **2020**, *56*, 216–225. [CrossRef]
34. Tlali, P.M.; Wang, R.-J.; Gerber, S.; Botha, C.D.; Kamper, M.J. Design and performance comparison of vernier and conventional pm synchronous wind generators. *IEEE Trans. Ind. Appl.* **2020**, *56*, 2570–2579. [CrossRef]
35. Cao, D.; Mecrow, B.; Deng, X.; Tavner, P.; Atkinson, G.; Shen, X.; Zhao, W. Conceptual design of different winding types for a 20mw wind turbine generator. In Proceedings of the 2022 7th International Conference on Environment Friendly Energies and Applications (EFEA), Moka, Mauritius, 14–16 December 2022; IEEE: Piscataway, NJ, USA, 2022. [CrossRef]
36. Abdel-Khalik, A.S.; Ahmed, S.; Massoud, A.M. Low space harmonics cancelation in double-layer fractional slot winding using dual multiphase winding. *IEEE Trans. Magn.* **2015**, *51*, 8104710. [CrossRef]
37. Zhao, W.; Zheng, J.; Ji, J.; Zhu, S.; Kang, M. Star and delta hybrid connection of a fscw pm machine for low space harmonics. *IEEE Trans. Ind. Electron.* **2018**, *65*, 9266–9279. [CrossRef]
38. Rudden, I.A.; Li, G.J.; Kana, D.K.; Zhu, Z.Q.; Duke, A.; Clark, R.; Thomas, A. Space harmonic cancellation in a dual three-phase spm machine with star-delta windings. *IEEE Trans. Energy Convers.* **2024**, *39*, 457–468. [CrossRef]
39. Rudden, I.A.; Li, G.J.; Kana Padinharu, D.K.; Zhu, Z.Q.; Duke, A.; Clark, R.; Thomas, A. General design rules for space harmonic cancellation in m-phase machines with n-converters and star-polygonal windings. *IEEE Trans. Energy Convers.* **2024**; *under review*.

40.   Yu, J.; Yang, J.; Dai, S.; Wang, Z.; Li, Q.; Huang, S.; Huang, S. Investigation on performance of multiple three-phase electrical machine with star–delta windings. *IEEE Trans. Ind. Electron.* **2023**, *71*, 8362–8372. [CrossRef]

41.   Magnussen, F.; Sadarangani, C. Winding factors and joule losses of permanent magnet machines with concentrated windings. In Proceedings of the IEEE International Electric Machines and Drives Conference, 2003. IEMDC'03, Madison, WI, USA, 1–4 June 2003; IEEE: Piscataway, NJ, USA, 2003. [CrossRef]